



Research Paper

Important Parameters of Ceramic Membranes Derived from Oasis Waste and Its Application for Car Wash Wastewater Treatment

Adel Zrelli ^{1,2,*}, Abdelbasset Jemai Bessadok ^{1,3}, Qusay Alsahy ⁴

¹ Higher Institute of Applied Sciences and Technology of Gabes, University of Gabes, 6072 Gabes, Tunisia

² Laboratory of Energy, Water, Environment, and Process, LR18ES35, National Engineering School of Gabes, University of Gabes, 6072 Gabes, Tunisia
Tel (00216) 75 39 21 08, Fax (00216) 75 39 23 90

³ Chemical Engineering Department, College of Engineering, King Saud University, P.O. Box 800, Riyadh 11421, Saudi Arabia

⁴ Membrane Technology Research Unit, Chemical Engineering, Department, University of Technology, Alsinaa Street No. 52, Baghdad 35010, Iraq

Article info

Received 2021-08-28

Revised 2021-10-28

Accepted 2021-11-09

Available online 2021-11-09

Keywords

Ceramic membrane

Oasis waste

Optimal fabrication parameters

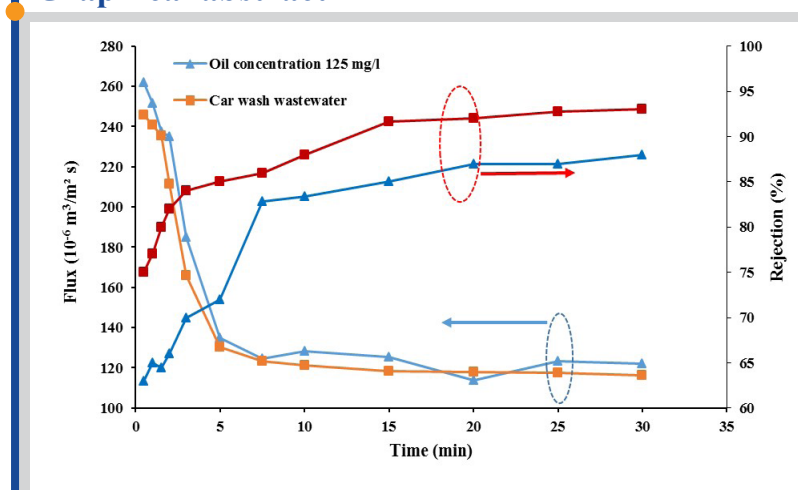
Characterization

Car wash wastewater treatment

Highlights

- Parametric study on ceramic membrane is presented.
- The influence of the incorporation of oasis waste is investigated.
- The treatment of simulated oily wastewater is studied.
- The performance of our ceramic membranes is discussed.

Graphical abstract



Abstract

The purpose of this study is to examine the best experimental parameters, which are the oasis waste concentration, molding pressure, and sintering temperature for the fabrication of ceramic membrane to be used in the treatment of car wash wastewater. These membranes were prepared from clay and oasis waste using the semidry-pressing process. Characterization of these membranes was carried out by the determination of their porosity, contact angle, and shrinkage. Following the experiments, we notice that when the oasis waste concentration goes from 8% to 22%, the membranes become more hydrophilic. The same evolution is observed when the sintering temperature and molding pressure increase from 700 to 900°C, and eight to 12 bars, respectively. Moreover, membrane porosity increases with the increase of sintering temperature and oasis waste concentration by 14.6% and 49.3%, respectively. In addition, permeate flux is proportional to the oasis waste concentration and the sintering temperature. The highest flux increase is 62.2% for the case of 15% of oasis waste concentration, while a drop of 23.8% for permeate flux is recorded with the rise of molding pressure. After determining the membrane specific volume, which complies with the Tunisian standards NT.106.002, the best experimental parameters for the membrane fabrication are found to be: (i) 22% of oasis waste concentration, (ii) 800°C for sintering temperature, and (iii) 8 bars for molding pressure. After 30 minutes of the experimentation of wastewater treatment of car wash using the best membrane, an oil rejection of 93% and permeate flux of $116 \times 10^{-6} \text{ m}^3/\text{m}^2\text{s}$ could be achieved.

© 2022 FIMTEC & MPRL. All rights reserved.

1. Introduction

Oily wastewater constitutes the most considerable quantity of liquid waste in the world. Consequently, it harms the environment and life quality of people. In addition, failure to recover such oil leads to a substantial economic

loss [1]. Oily wastewater is widely emanating from several industrial origins such as petrochemical, pharmaceutical, metal, or food industries. It has been found that the main compounds of these various oily wastewaters are oil, grease, and surfactants.

* Corresponding author: adel.zrelli@yahoo.fr (A. Zrelli)

Although oily wastewater treatment has been performed by different techniques such as air flotation [2], coagulation [3], electroflotation [4]. According to the study of Al Adetunji et al. [5], these conventional methods have their disadvantages which include high operational cost and low treatment efficiency.

The most used techniques are membrane processes. In these processes, choosing the best membrane is crucial to have a high efficiency of the oily wastewater treatment process. Generally, membrane can be used in distillation [6,7], and in filtration unit operations [8].

Membranes are generally fabricated from polymeric and ceramic materials. Ceramic membranes are more robust in terms of chemical and mechanical resistance, and are used in a wide range of temperatures. Nevertheless, ceramic membrane has the drawbacks of low selectivity and high cost of fabrication [9,10]. The ceramic membrane cost can be reduced by using local products such as local clay, pore-forming, plasticizers, etc. [11]. The characteristics of a ceramic membrane can be facilitated by optimization of the fabrication operating parameters. Many studies revealed that the addition of organic waste plays the role of a pore-forming [12–14]. Based on a study conducted by Ben Ali et al., the use of olive pomace as pore-forming promoted both the porosity and the permeability of the ceramic membrane. For a membrane sintered at 1000°C, when the olive pomace concentration had changed from 20% to 30% the porosity increased by 37% and the permeability by 252%. According to Kumar et al. [15], a small pore size induces an increase in oil rejection from the oily wastewater. This rise of rejection induces the increase of the membrane fouling and the concentration polarization.

Animesh et al. [16] noted that a lower pore size (20–42 nm) of the ceramic membrane undergoes significant fouling through pore-blocking and not by the formation of a cake layer. However, the larger pore size (3–7 µm) of the ceramic membrane facilitates the formation of a cake layer. Based on Darcy's law, when transmembrane pressure increases, the permeate flux increases as well [17]. Nevertheless, a decrease in oil rejection can be remarked with this increase in transmembrane pressure. This decrease can be explained by the fact that increasing the transmembrane pressure, forces the oil droplets to pass through the membrane pore and to be on the permeate side [18]. After optimization of this transmembrane pressure, to have a high permeate flow value with tolerable oil rejection, an increase in the efficiency of the oily wastewater treatment process is observed [5]. For example and in the case of a transmembrane pressure of 68.95 kPa, the oil rejection was about 98.9% and the permeate flux was $5.36 \cdot 10^{-6} \text{ m}^3/\text{m}^2\text{s}$.

In addition, the choice of the best surface membrane charge leads to better filtration performance [19]. When the oil droplets and the membrane surface are charged oppositely, the obtained permeate flux tends to be high but marked by a low rate of oil rejection. On the other hand, for the same charge of membrane surface and oil droplets, a strong decrease in the permeate flux was observed, with a moderate rejection of oil.

The current study presents the role of effective parameters such as molding pressure, sintering temperature, and oasis waste concentration on the ceramic membrane performance. The best fabrication parameters can be found based on the appropriate membrane performance during car wash wastewater treatment. To our knowledge, no study has so far been reported on the influence of the three parameters of molding pressure, sintering temperature, and oasis waste concentration on ceramic membrane performances.

2. Material and method

2.1. Ceramic membrane preparation

The ceramic membranes are prepared using the semidry-pressing process [20]. First, clay and oasis waste were dried to a constant weight. After grinding dry oasis waste to uniform particle sizes using a laboratory grinder (Retsch SM 100), particle size distribution is performed by the collection of particle size fractions between 63 and 80 µm. These same operations are executed for the clay, by crushing in a Matest A092 brand grinder. Clay and oasis waste particles are then mixed at a predetermined ratio (Table 1) until obtaining a homogeneous state. Then, 20% deionized water is added to the dry mixture to obtain a suitable paste for molding. The obtained paste is then treated for 30 minutes by ultrasonic to prevent the formation of air bubbles and consequently avoid membrane cracks during the sintering step. After that, this paste was kept at rest for 24 hours at room temperature and pressed using Edibon EEU/20KN press at different pressure in cylindrical samples 3mm in thickness and 55mm in diameter. After pressing, these samples were kept at rest for 24 hours at room temperature and sintered in a laboratory Nabertherm furnace at a temperature of 700, 800, and 900°C.

Table 1
Parameters for the membranes preparation.

Membrane	M1	M2	M3	M4	M5	M6	M7
Molding pressure (bar)	8	10	10	12	8	8	10
Sintering temperature (°C)	800	700	900	800	800	800	800
Oasis waste (%)	22	22	22	22	8	15	22

2.2. Membranes characterization

2.2.1. Chemical characterization

Fourier transform infrared (FTIR) analysis of the samples was carried out using Spectrum Two (PerkinElmer, USA) FTIR spectrometer. The spectrometer was equipped with a diamond attenuated total reflectance (ATR) accessory. Spectra were recorded in the wavenumbers range of 450–4000 cm^{-1} by an average of 4 scans at a spectral resolution of 2 cm^{-1} . In addition, x-ray diffractometry (XRD) analysis was performed using a Siemens Bruker X-ray diffractometer equipped with Cu K α radiation. Typically θ -2 θ spectra were collected between $2\theta=10^\circ$ and 70° in 0.02° steps. The characterization of the oasis waste was presented in our previous work [21].

2.2.2. Membrane porosity

Membrane porosity was determined according to the Archimedes method [21,22]. Using this method, the effects of sintering temperature, molding pressure, and oasis waste addition on this membrane porosity can be explored.

2.2.3. Contact angle

The membrane hydrophobicity (hydrophilicity) can be determined by the contact angle measurement performed with KRÜSS Drop Shape Analyzer – DSA25. The contact angle was determined using Advance software.

2.2.4. Liquid Entry Pressure (LEP)

LEP characterizes the limit of pressure applied on the feed side of the membrane before the liquid water enters through the membrane's pores. LEP can be calculated by the following expression [23]:

$$LEP = \frac{B\gamma_L \cos\theta}{d_{max}} \quad (1)$$

Where B is the pore factor of geometry, θ is the contact angle ($^\circ$), γ_L is the surface tension of water (N/m), and d_{max} is the diameter maximum of pores (μm).

2.2.5. Oily wastewater treatment

We used a dead-end unit to characterize and treat the car wash wastewater (Figure 1). In this unit, we fixed the ceramic membrane at the bottom. After, we forced by compressed air the car wash wastewater to pass through this membrane. Then, we weigh the obtained permeate, and we determine the oil concentration by UV-visible spectrophotometry (PG instruments T 80 spectrophotometer) at a wavelength of 235 nm.

3. Results and discussion

3.1 Clay characterization

The FT-IR peaks assignments were based on the works of Saikia et al. [24], and Kamgang-Syapnjeu et al. [25]. The band observed at around 3620 cm^{-1} (Figure 2) has been ascribed to OH stretching. The peak assigned to the H–O–H bending of water can be shown at around 1636 cm^{-1} . The peak located at 1007 cm^{-1} was attributed to symmetrical and asymmetrical elongation vibrations of the Si–O–Si bond. Peak obtained at around 798 cm^{-1} assigned to OH deformation linked to Mg^{2+} and Al^{3+} .

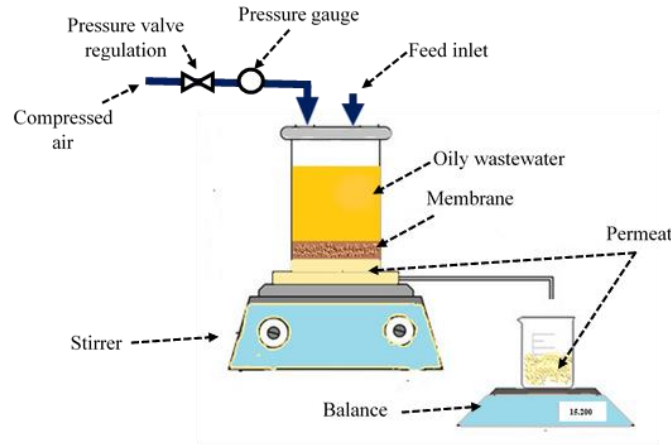


Fig. 1. The dead-end unit used in characterization and car wash wastewater treatment.



Fig. 2. The spectrum of the clay powder.

The vibration band observed at 919 cm^{-1} corresponds to the deformation of the Al-OH bond, while the other one observed at 693 cm^{-1} corresponds to the different modes of the Si-O-Al bond. The peak towards 524 cm^{-1} is assigned to Si-O-Al bending vibrations. The peak observed at around 466 cm^{-1} is assigned to Si-O-Si bending. The presence of Si-O-Si, OH groups, Si-O-Al, and Al-OH peaks can be referred to the presence of kaolinite at the angles $2\theta=12.42^\circ$ and $2\theta=29^\circ$ and illite at the angles $2\theta=20^\circ$ and $2\theta=50^\circ$ shown by XRD in Figure 3.

Based on X-ray fluorescence, the chemical composition of the used clay expressed in mass percentages is given in Table 2.

According to Table 2, the clay contains a higher percentage of calcium oxide, silicon dioxide, and aluminum oxide while it contains a low percentage of ferric oxide, magnesium oxide and potassium oxide.

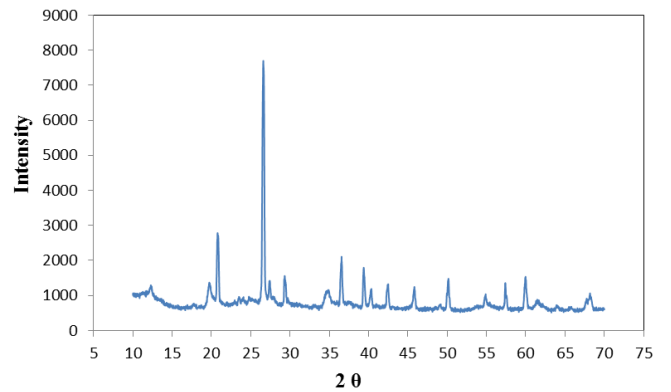


Fig. 3. X-ray diffraction of clay.

Table 2
Clay composition.

Composition (%)	CaO	SO ₃	SiO ₂	P ₂ O ₅	Al ₂ O ₃	FeO ₃	K ₂ O	MgO
Clay	11	-	37.75	-	15	4	1.1	5

3.2. Parametric study of the obtained membranes

3.2.1. Effect of sintering temperature on open porosity

To present the effect of sintering temperature on open porosity, the molding pressure was fixed at 10 bars, while the sintering temperature was varied between 700°C and 900°C. The obtained results of ceramic membrane open porosity are presented in Figure 4. According to Figure 4, when the oasis waste varies from 8% to 22%, an increase in the open porosity for all sintering temperatures was observed. This increase has two slopes marked by a rapid evolution from 8% to 11% of oasis waste and a slow evolution for the last part. For the case of 900°C, open porosity varied from 26.1% to 43.3% with this evolution of oasis waste. Additionally, the open porosity increases with the increase of the sintering temperature. This variation is due to the opening of pores and the volatilization of the oasis waste ash with the increase in sintering temperature. The same finding has been presented by Kamoun et al. [26].

3.2.2. Effect of molding pressure on open porosity

The effects of a molding pressure of 8, 10, and 12 bars on ceramic membrane open porosity were studied at a constant sintering temperature of 800°C. The experimental results are shown in Figure 5. This figure shows that a greater impact of the molding pressure on the open porosity can be remarked. As can be seen, open porosity was gradually decreased for all different amounts of oasis waste. For example, when the molding pressure grows from 8 to 12 bars, for an amount of oasis waste of 22%, a decrease by 13.62% of the open porosity can be observed. This decrease can be interpreted by the fact that when the molding pressure increases, the void between the particles is reduced leading to a reduction of the internal pores and porosity after sintering.

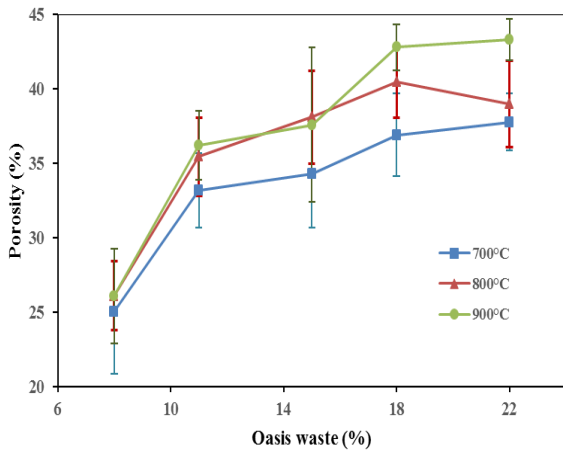


Fig. 4. Variation of open membrane porosity with oasis waste percentage at a molding pressure of 10 bars and for different sintering temperatures.

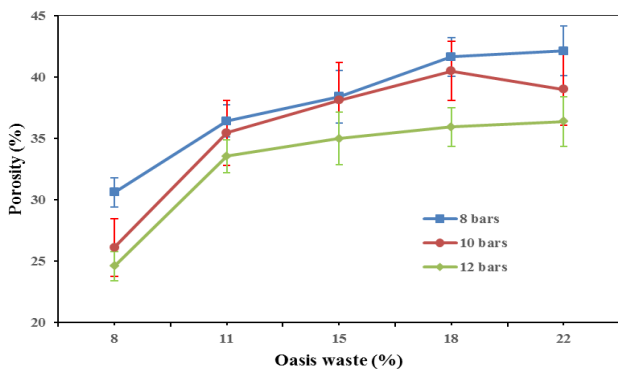


Fig. 5. Variation of membrane open porosity with oasis waste percentage at a sintering temperature of 800°C and for different molding pressures.

3.2.3. Effect of oasis waste percentage on open porosity

When the oasis waste concentration was varied from 8% to 15% (Figure 6), at a sintering temperature of 800°C and molding pressure of 8 bars, a sharp increase of the open porosity of the prepared ceramic membrane from 26.12% to 40.05% was observed. For this same evolution of oasis waste, a slight variation of the closed porosity was detected. Following that, no effect of adding oasis waste to the solid phase of ceramic membrane on open porosity was noted. Nevertheless, an increase of closed porosity could be observed. In this case, the oasis waste was combined in an aggregate and the number of aggregate increases with the increase of the oasis waste percentage. After combustion, these aggregates lead to a closed porosity.

3.2.4. Effect of molding pressure on contact angle

Figure 7 presents the evolution of the contact angle of ceramic membranes as a function of oasis waste percentage and at three molding pressure. According to Figure 7, the prepared membranes have hydrophilic surfaces. Additionally, a decrease in the contact angle is shown with the increase of the molding pressure for all percentages of oasis waste. According to Gu et al. and Usman et al. [27,28], the surface energy, chemical composition, and surface roughness influence the membrane contact angle. In this study, this evolution can be explained by the fact that the increase in the molding pressure induces an increase in the compactness of the membrane and a decrease in surface roughness and consequently in the contact angle.

3.2.5. Effect of sintering temperature on contact angle

Figure 8 illustrates the variation of the contact angle as a function of oasis waste percentage and at three sintering temperatures 700, 800, and 900°C. In these evolutions, the molding pressure was fixed at a constant value equal to 10 bars. As it can be seen, a decrease of ceramic membrane contact angle with the increase of the sintering temperature is observed. Increasing the sintering temperature increases the quantity of liquid phase obtained during the evolution of the sintering process. This liquid phase leads to obtaining a membrane surface that is less rough and therefore more hydrophilic [29].

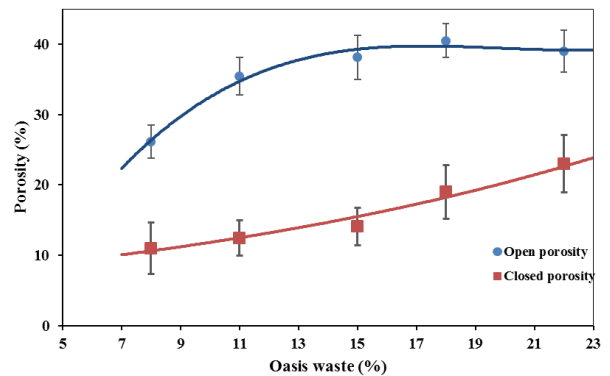


Fig. 6. Evolution of membrane open and closed porosity with oasis waste percentage at 800°C of sintering temperature and a molding pressure of 10 bars.

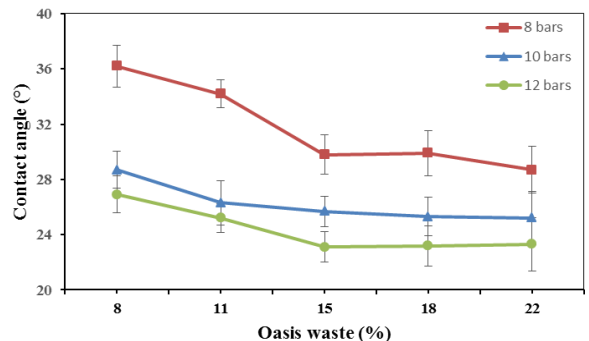


Fig. 7. Variation of contact angle of ceramic membranes with oasis waste at different molding pressure 8, 10, and 12 bars.

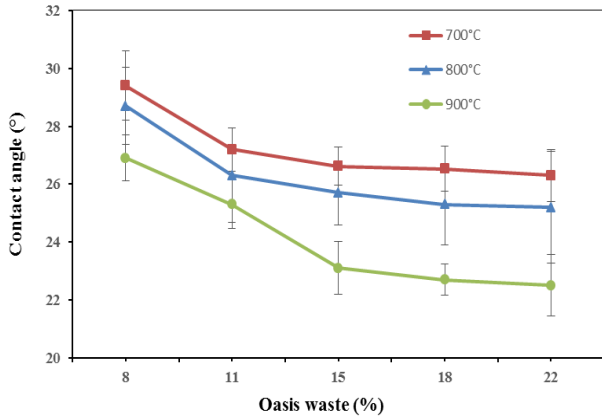


Fig. 8. Contact angle of ceramic membranes versus oasis waste percentage for ceramic membrane sintered at 700, 800, and 900°C.

3.2.6. Effect of oasis waste percentage on contact angle

To see the effect of oasis waste concentration on the membrane contact angle, used as a porogen agent, this concentration was varied from 8% to 22%. Figure 9 presents the obtained results of the contact angle. According to Figure 9, our membranes have a hydrophilic characteristic. This characteristic tends to become more and stronger with the increase of the oasis waste concentration in the solid phase of the ceramic membrane. The variation of the contact angle with the oasis waste concentration showed two slopes. The first slope is a decrease of contact angle with the adding of oasis waste concentration from 8% to 15%. After this value, no effect of adding oasis waste on the contact angle can be remarked. This evolution can be explained by the increase in the membrane open porosity with the increase of the oasis waste (see Figure 4). This increase in porosity leads to a strong tendency for water to spread and rapidly absorbed by the membrane surface.

3.2.7. Effect of sintering temperature on volume shrinkage

Figure 10 exhibits the shrinkage percentage of the prepared ceramic membranes at different sintering temperatures. According to Figure 10, membrane shrinkage was found to rise with an increase in sintering temperature for all ranges of oasis waste. For example, in the case of 22% oasis waste, when the sintering temperature grows from 700 to 900°C, membrane shrinkage increases by 13%. According to Salman et al. and Harun et al. [30,31], the shrinkage of the prepared ceramic membranes during the sintering process occurs mainly due to moisture loss. With the increase of sintering temperature, the amount of losses moisture rises which induces more void between solid-phase particles. In addition, a rise in the liquid phase quantity with the increase of sintering temperature can be remarked. This quantity of liquid phase fills part of the formed voids and reduces the membrane volume, increasing shrinkage with sintering temperature.

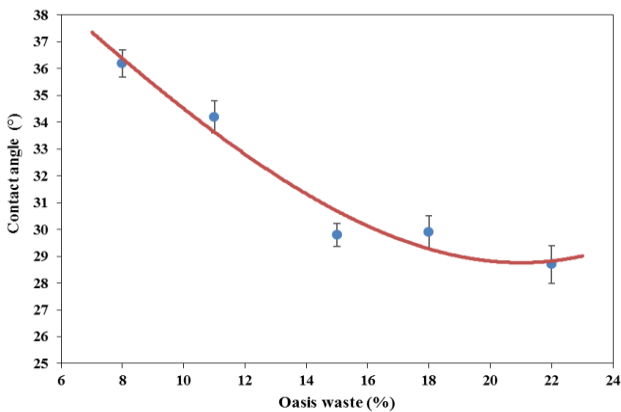


Fig. 9. Evolution of contact angle with oasis waste percentage.

3.2.8. Effect of molding pressure on volume shrinkage

Figure 11 presents the effect of molding pressure on ceramic membrane shrinkage. According to Figure 11, a significant decrease in shrinkage with an increase in molding pressure for all oasis waste percentages can be observed. When the molding pressure was increased from 8 bars to 12 bars, a drop in shrinkage of 19% for 22% of the oasis waste was observed. Based on Figure 5 a decrease in porosity with the increase of molding pressure, the molten part of the solid phase finds less void between the particles, due to the pressure increase, and less shrinkage can be obtained. In this case, a deformation of the membrane can be observed. The same results have been obtained by Harun et al., Suvorova et al. and Mankai et al. [31–33].

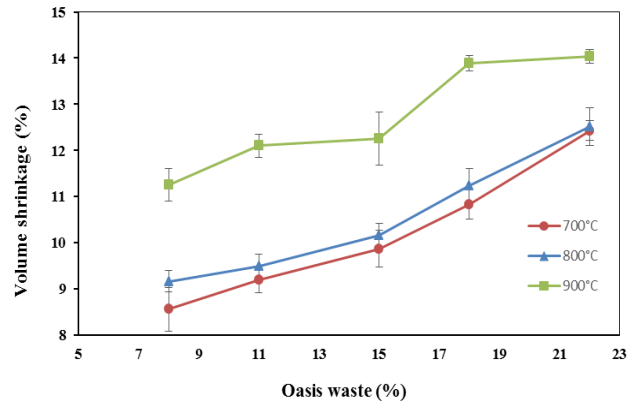


Fig. 10. Shrinkage percent of ceramic membranes versus oasis waste percentage for ceramic membrane sintered at 700, 800, and 900°C.

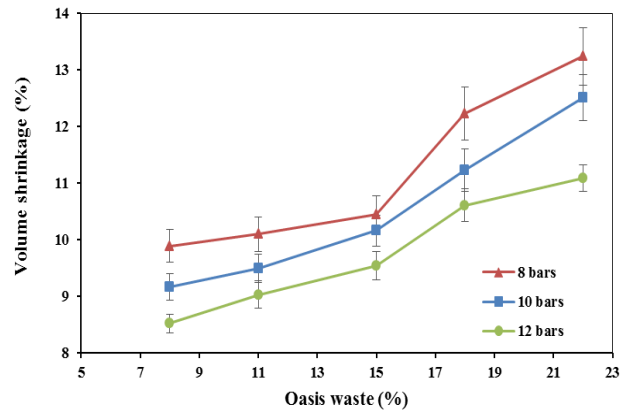


Fig. 11. Evolution of volume shrinkage with molding pressure for different oasis waste percentages and at 800°C.

3.3. Treatment of oily wastewater

Figure 12 shows the evolution of permeate flux for 125 mg/l oil feed concentration and the percent rejection with time. It can be observed from this figure that there is a decrease of the permeate flux with the increase of time. This permeate flux has greatly diminished during the first 5 to 10 minutes of operation and gradually becomes steady subsequently. This decrease may be related to the fouling phenomenon marked by the blockage of the ceramic membrane pores by the oil droplets and the formation of the thin layer of oily film on the surface of the membrane. Besides, the permeate flux increases when the oasis waste concentration rises from 8% to 15% (Figure 12a) due to the increase in porosity from 30.62% to 38.4%. From 15% to 22% of the oasis waste, a decrease of permeate flux can be remarked due to the membranes pore size decrease from 3.44 to 2.32 μm (Table 3). Also, the permeate flux decreases with the increase of sintering temperature (Figure 12b). This evolution is due to the difference in the porosity of the prepared ceramic membranes in the various sintering temperature. From Figure 12b and at the

time of 30 minutes, a decrease of permeate flux from $115.7 \cdot 10^{-6}$ to $99.39 \cdot 10^{-6} \text{ m}^3/\text{m}^2 \text{ s}$ was observed with the increase of sintering temperature from 700 to 900°C. Increasing temperature from 700 to 900°C increases the liquid phase quantity formed throughout the sintering process. This liquid phase penetrates the pores and reduces the pore diameter [34]. In addition, an increase in the pore number due to the volatilization of oasis waste ash with the sintering temperature increase. These two findings, of an increase in the number of pores and a reduction in the diameter of these pores, induce a reduction in the permeate flux.

A decrease in permeate flux was observed with the increase of molding pressure from 8 bars to 12 bars for all periods of experimentation (Figure 12c). This decrease can be linked to the reduction of porosity with the increase of molding pressure presented in Figure 5, which can be attributed to the reduction of the void between the particles. At the same time, this decrease was about 30% at 0.5 min and 20% at 30 minutes. This last evolution can be related to the increase of the fouling phenomenon with time marked by pore blocking and the increase of the polarization concentration layer [35].

Table 3

Properties of prepared ceramic membranes at sintering temperature of 800°C and molding pressure of 8 bars.

Oasis waste (%)	LEP (kPa)	θ (°)	ϵ (%)	d_{max} (µm)
8	8.00	36.20	30.62	1.60
15	4.00	29.80	38.41	3.44
22	6.00	28.70	42.12	2.32

LEP: liquid entry pressure; θ : contact angle; ϵ : open porosity; and d_{max} : maximum pore diameter

Figure 12a shows the evolution of rejection with the increase in time and for three oasis waste concentrations. For all these concentrations, the rejection increases with the increase of time. For the case of 15% of oasis waste concentration, the rejection of the membrane rises by 35% with the increase in time from 0.5 to 30 minutes. This increase of membrane rejection with time can be related to the fouling phenomenon and principally to the membrane pore diameter reduction because of the oil droplets adsorption in the membrane pores. Moreover, the membrane prepared with 15% of oasis waste presents less value of rejection. This result can be explained by the fact that this membrane has a high value of pore diameter (see Table 3), which allows some droplets of oil to pass via these pores and reach the permeate side.

The effect of sintering temperature on oil rejection with time is shown in Figure 12b. For all experiments, the oil rejection is in the range of 61.53 to 94.39%. It was observed that the sintering temperature at 700°C had lower oil rejection. Moreover, with the rise of sintering temperature, the oil rejection increases. At 30 minutes, an increase in oil rejection of about 11% is noticed when the sintering temperature goes from 700 to 900 °C. A decrease in membrane pore size is observed at higher temperature, limiting oil droplets from passing through the membrane, resulting in an increased oil rejection.

Rejection of oil for different molding pressures is shown in Figure 12c. The oil rejection increased with the increase of molding pressure for the time of experimentation. This variation may be due to a decrease in the void between particles with the molding pressure increase inducing to decrease in pore diameter and contact angle (see Figure 7) and an increase in hydrophilicity and oil rejection.

According to the Tunisian standard relating to effluent discharges into the water environment NT. 106.002, the discharge into the aquatic environment of treated wastewater from the car washes is considered safe if their oil concentration is less than 20 mg/l [36]. In the presented experiments, a feed with an oil concentration of 125 mg/l has been used. This oil concentration corresponds to a minimal authorized value of oil rejection of 84%. Based on this value, we can determine the specific permeate volume treated by each prepared membrane in which the oil concentration is below the Tunisian standard. Next, the obtained results are presented in Figure 13. According to Figure 13, the permeate of the membranes M3 and M6 do not comply with the Tunisian standard NT. 106.002. Moreover, only membranes M1 and M2 exhibit high specific volume values with excess for M1.

Figure 14 presents the effect of feed oil concentration on permeate flux and oil rejection. For the experiment time and the three feed oil concentrations, a decrease of permeate flux with an increase of feed oil concentration could be observed. For the case of oil concentration 125 mg/l, permeate flux decreased by 53%. Moreover, increasing the feed oil concentration from 125 to 500 mg/l leads to a decrease in the flux of about 67% and 76% at 0.5 minutes and 30 minutes, respectively. The decline of permeate flux with an increase of feed oil concentration can be related to the increase in the polarization concentration layer formed by the rejected oil on the membrane surface. For the case of oil rejection and at the time of the experiment, an increase of about 39% and 30% for oil feed concentrations of 125 mg/l and 500 mg/l were observed, respectively. Furthermore, we notice an increase in oil rejection with the feed oil concentration increase. This increase is due to the oil droplet coalescence inducing an increase in droplet size and fouling phenomena and consequently the oil rejection.

3.4. Treatment of car wash wastewater

Car wash wastewaters were collected from five stations situated in the city of Gabes, Tunisia. These stations were specialized in car washing and oil drainage activities. Table 4 summarizes the used car wash wastewater characteristics. Sedimentation and filtration were used as a pretreatment of the car wash wastewater sample. First, sedimentation for 1 hour [37] was used to remove the solid particles dispersed in this wastewater. Then, using a filter

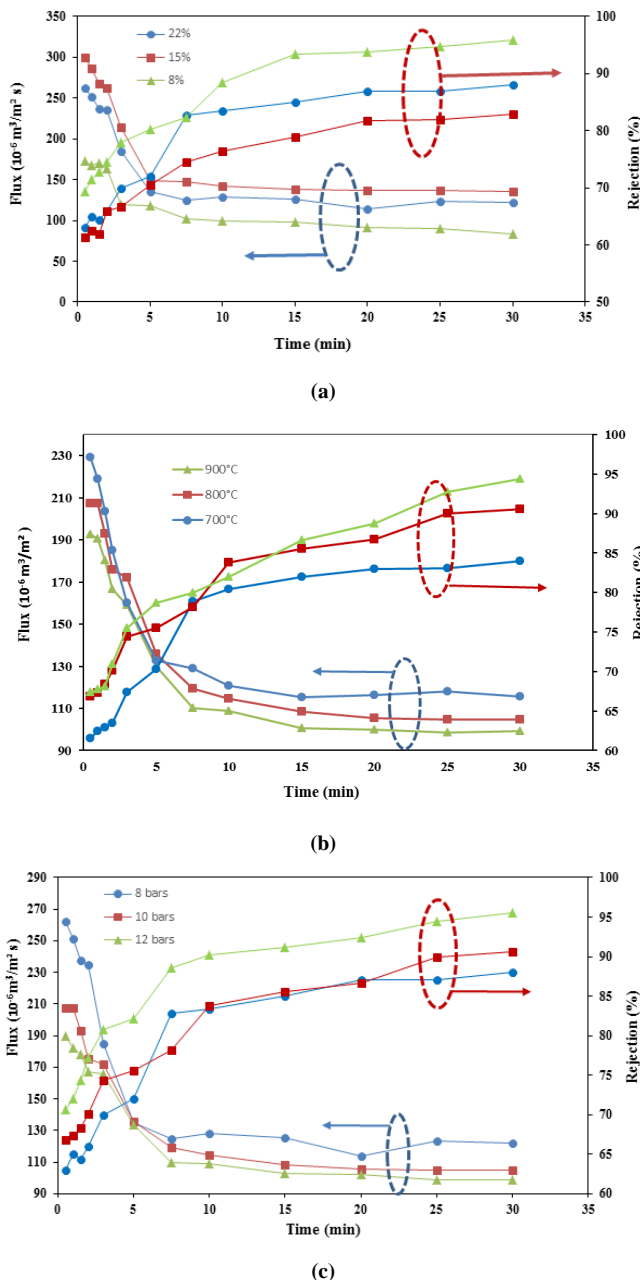


Fig. 12. Variation of permeate flux and oil rejection efficiency with time at different (a) oasis waste concentration; (b) sintering temperature (c); molding pressure.

paper, the obtained wastewater was filtered, with less quantity of solid particles, to minimize the floating oil. These two steps are so essential to reduce the increase of fouling phenomena and decrease of the treatment efficiency [38,39]. After, the resulting car wash wastewater was treated with the dead-end filtration unit presented by Figure 1. In this case, a ceramic membrane was used with 22% of oasis waste, molded at 8 bars and sintered at 800°C. The evolution of permeate flux and oil rejection with time are presented in Figure 15. This figure shows a decrease of the permeate flux with the increase of time. In addition, comparing the evolution of the flux for the feed with oil concentration of 125 mg/l to that for the car wash wastewater, a slighter decrease was noticed (about 5%) for the case of car wash wastewater. This decrease can be related to an increase of the fouling phenomena for this type of wastewater.

Moreover, with respect to the oil rejection, an increase can be observed for the car wash wastewater. This increase is about 19 % at 0.5 minutes and 5% at 30 minutes. These two remarks can be explained by the fact that in the wash car station, they use detergent composed of surfactant, which interacts with the membrane surface to provide less flux reduction and better oil rejection [40]. The results obtained for the case of oil rejection of our ceramic membranes are in line with similar results from other studies. Table 5 presents a comparison between our obtained results and the results of other researches.

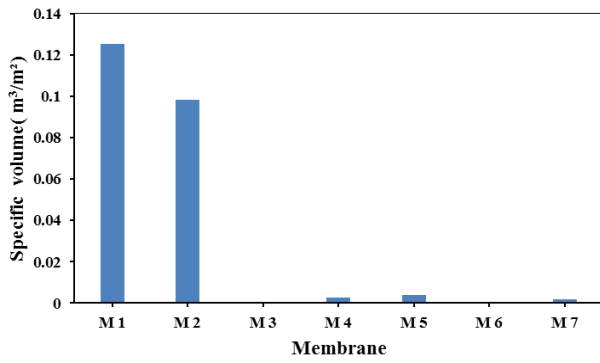


Fig. 13. Variation of specific volume for different membranes.

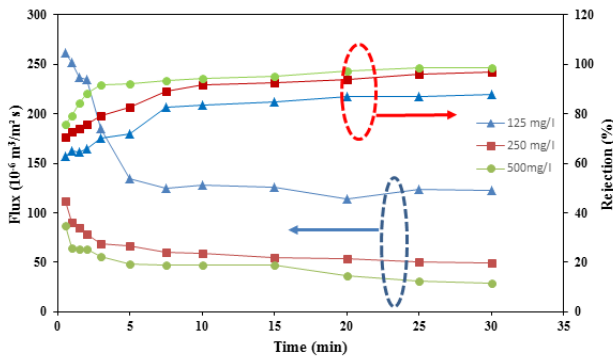


Fig. 14. Variation of permeate flux and oil rejection efficiency with time at different oil concentration.

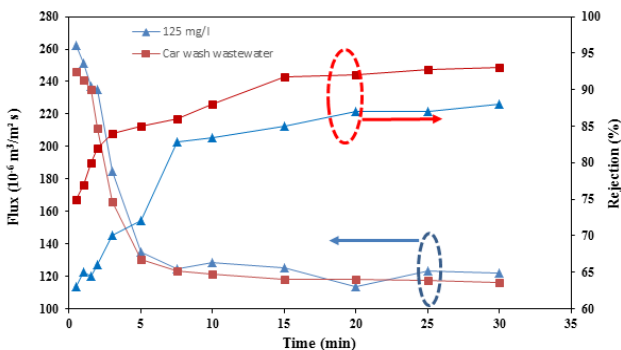


Fig. 15. Evolution of permeate flux and oil rejection efficiency with time for oil concentration 125 mg/l and car wash wastewater.

Table 4 Characteristics of car wash wastewater.

Parameter	Total solids (mg/l)	pH	Conductivity (µs/cm)	Oil content (mg/l)
Value before treatment	1115	7.5	915	137
Value after treatment	572	7.8	412	9.59

Table 5 Comparison of obtained results with other results from literature.

Major raw material	Pore size (µm)	Sintering temperature (°C)	Oil rejection (%)	Permeate flux (l/hm²)	Ref.
α-Alumina oxide, Zirconia oxide and titanium oxide	0.02	1400	78	100	[41]
Sugarcane and bagasse ash	7.5	1000	95.7	87.4	[42]
Clay and α-Alumina	0.289	1250	93.8	72.7	[43]
Kaolin and PEG	0.21	1500	99.99	320	[44]
Clay and SiC	1.3	1700	99.9	64.4	[45]
Clay and oasis waste	2.32	800	93	418.644	This study

4. Conclusions

In the present work, the effects of sintering temperature, molding pressure, and oasis waste concentration on the characteristics of prepared ceramic membranes have been studied. After experimentation, an increase of the porosity by 14.6% was observed when the sintering temperature was increased from 700 to 900°C. For this evolution of sintering temperature, a decrease of 16.9% for the contact angle and 16.4% for the permeate flux were recorded. However, an increase in oil rejection by 12.4% was noticed. Besides, when the molding pressure was varied from 8 to 12 bars, contact angle, porosity, and permeate flux decreased by 23.2%, 15.7%, and 23.8%, respectively. However, an increase in oil rejection by 8.6% could be observed. Moreover, when the oasis waste concentration changes from 8% to 22%, a rise of porosity by 49.3% and permeate flux by 62.2% were recorded. In addition, for this evolution of oasis waste concentration, a drop of about 26.2% for the contact angle and about 15.6% for oil rejection have been observed. For the case of the use of the prepared membrane in the field of car wash wastewater treatment, an oil rejection of about 93% was obtained, and the oil concentration of the permeate complies with the Tunisian standard NT. 106.002. In perspective, this work can further be carried out by determining the fouling phenomena model and the long-term use of our prepared membranes.

References

- [1] H.J. Tanudjaja, C.A. Hejase, V.V. Tarabara, A.G. Fane, J.W. Chew, Membrane-based separation for oily wastewater: A practical perspective, *Water Res.* 156 (2019) 347–365. <https://doi.org/10.1016/j.watres.2019.03.021>
- [2] T.J. Mohammed, S.S. Mohammed, Z. Khalaf, Treatment of oily wastewater by induced air flotation, *Eng. Technol. J.* 31 (2013).
- [3] X.-N. Cheng, Y.-W. Gong, Treatment of oily wastewater from cold-rolling mill through coagulation and integrated membrane processes, *Environ. Res.* 23 (2018) 159–163. <https://doi.org/10.4491/er.2016.134>
- [4] A. Genç, S. Goc, Electroflotation of oily wastewater using stainless steel sponge electrodes, *Water Sci. Technol.* 78 (2018) 1481–1488. <https://doi.org/10.2166/wst.2018.422>
- [5] A.A. Isiaka, A.O. Olaniran, Treatment of industrial oily wastewater by advanced technologies: a review, *Appl. Water Sci.* 11 (2021). <https://doi.org/10.1007/s13201-021-01430-4>
- [6] A. Zrelli, B. Chaouachi, S. Gabsi, Simulation of a solar thermal membrane distillation: Comparison between linear and helical fibers, *Desalination Water Treat.* 52 (2014) 1683–1692. <https://doi.org/10.1080/19443994.2013.807033>

- [7] A. Zrelli, B. Chaouchi, S. Gabsi, Use of solar energy for desalination by membrane distillation installation equipped with helically coiled fibers, in: IREC2015 Sixth Int. Renew. Energy Congr., IEEE, 2015: pp. 1–4. <https://doi.org/10.1109/IREC.2015.7110893>
- [8] R. Ben Amar, M. Khemakhem, A. Oun, S. Cerneaux, M. Cretin, S. Khemakhem, Decolorization of Dyeing Effluent by Novel Ultrafiltration Ceramic Membrane from Low Cost Natural Material, *J. Membr. Sci. Res.* 4 (2018) 101–107. <https://doi.org/10.22079/JMSR.2017.69818.1154>
- [9] J. López, M. Reig, X. Vecino, O. Gibert, J.L. Cortina, Comparison of acid-resistant ceramic and polymeric nanofiltration membranes for acid mine waters treatment, *Chem. Eng. J.* 382 (2020) 122786. <https://doi.org/10.1016/j.cej.2019.122786>
- [10] S.S. Wadekar, R.D. Vidic, Comparison of ceramic and polymeric nanofiltration membranes for treatment of abandoned coal mine drainage, *Desalination*. 440 (2018) 135–145. <https://doi.org/10.1016/j.desal.2018.01.008>
- [11] H. Nasri, S. Khemakhem, R.B. Amar, Physico-chemical study of coating formulation based on natural apatite for the elaboration of microfiltration membrane, *Period. Polytech. Chem. Eng.* 58 (2014) 171–178. <https://doi.org/10.3311/PPCh.7388>
- [12] F.A.M. Rahim, M.Z. Noh, M.W.A. Rashid, J.J. Mohamed, M.A.A.M. Nor, Preparation and characterization of ceramic membrane by using palm fibers as pore forming agent, in: AIP Conf. Proc., AIP Publishing LLC, 2019: p. 020056. <https://doi.org/10.1063/1.5089355>
- [13] W. Misrar, M. Loutou, L. Saadi, M. Mansori, M. Waqif, C. Favotto, Cordierite containing ceramic membranes from smectitic clay using natural organic wastes as pore-forming agents, *J. Asian Ceram. Soc.* 5 (2017) 199–208. <https://doi.org/10.1016/j.jascer.2017.04.007>
- [14] A.I. Ivanets, T.A. Azarova, V.E. Agabekov, S.M. Azarov, C. Batsukh, D. Batsuren, V.G. Prozorovich, A.A. Rat'ko, Effect of phase composition of natural quartz raw material on characterization of microfiltration ceramic membranes, *Ceram. Int.* 42 (2016) 16571–16578. <https://doi.org/10.1016/j.ceramint.2016.07.077>
- [15] S. Kumar, B.K. Nandi, C. Guria, A. Mandal, Oil removal from produced water by ultrafiltration using polysulfone membrane, *Braz. J. Chem. Eng.* 34 (2017) 583–596. <https://doi.org/10.1590/0104-6632.20170342s20150500>
- [16] A. Jana, S. Ghosh, S. Majumdar, Energy efficient harvesting of *Arthrospira* sp. using ceramic membranes: analyzing the effect of membrane pore size and incorporation of flocculant as fouling control strategy, *J. Chem. Technol. Biotechnol.* 93 (2018) 1085–1096. <https://doi.org/10.1002/jctb.5466>
- [17] A. Almojily, D.J. Johnson, S. Mandale, N. Hilal, Optimisation of the removal of oil in water emulsion by using ceramic microfiltration membrane and hybrid coagulation/sand filter-MF, *J. Water Process Eng.* 27 (2019) 15–23. <https://doi.org/10.1016/j.jwpe.2018.11.007>
- [18] A. Golshenas, Z. Sadeghian, S.N. Ashrafzadeh, Performance evaluation of a ceramic-based photocatalytic membrane reactor for treatment of oily wastewater, *J. Water Process Eng.* 36 (2020) 101186. <https://doi.org/10.1016/j.jwpe.2020.101186>
- [19] H. Nagasawa, T. Omura, T. Asai, M. Kanezashi, T. Tsuru, Filtration of surfactant-stabilized oil-in-water emulsions with porous ceramic membranes: Effects of membrane pore size and surface charge on fouling behavior, *J. Membr. Sci.* 610 (2020) 118210. <https://doi.org/10.1016/j.memsci.2020.118210>
- [20] Y. Feng, Z. Zhuang, Q. Zeng, D. Liu, Porous Ceramic-Based Metal–Organic Framework DBPC@ ZIF-67 for the Efficient Removal of Congo Red from an Aqueous Solution, *Cryst. Growth Des.* (2021). <https://doi.org/10.1021/acs.cgd.1c00529>
- [21] A. Zrelli, W. Elfalleh, A. Ghorbal, B. Chaouchi, Valorization of date palm wastes by lignin extraction to be used for the improvement of polymeric membrane characteristics, *Period. Polytech. Chem. Eng.* (2021). <https://doi.org/10.3311/PPCh.18273>
- [22] Q.F. Alsally, S.S. Ibrahim, F.A. Hashim, Experimental and theoretical investigation of air gap membrane distillation process for water desalination, *Chem. Eng. Res. Des.* 130 (2018) 95–108. <https://doi.org/10.1016/j.cherd.2017.12.013>
- [23] H. Ajari, A. Zrelli, B. Chaouchi, M. Pontié, Preparation and Characterization of Hydrophobic Flat Sheet Membranes Based on a Recycled Polymer, *Int. Polym. Process.* 34 (2019) 376–382. <https://doi.org/10.3139/217.3717>
- [24] J. Saikia, S. Sarmah, J.J. Bora, B. Das, L.R. Goswamee, Preparation and characterization of low cost flat ceramic membranes from easily available potters' clay for dye separation, *Bull. Mater. Sci.* 42 (2019) 104. <https://doi.org/10.1007/s12034-019-1767-7>
- [25] P. Kamgang-Syapnjev, D. Njoya, E. Kamseu, L.C. de Saint Cyr, A. Marciano-Zerpa, S. Balme, M. Bechelany, L. Soussan, Elaboration of a new ceramic membrane support from Cameroonian clays, coconut husks and eggshells: Application for *Escherichia coli* bacteria retention, *Appl. Clay Sci.* 198 (2020) 105836. <https://doi.org/10.1016/j.clay.2020.105836>
- [26] N. Kamoun, W. Hajjeji, R. Abid, M.A. Rodriguez, F. Jamoussi, Elaboration and properties of low-cost ceramic microfiltration membrane from local Tunisian clay for wastewater treatment, *Cerâmica*. 66 (2020) 386–393. <https://doi.org/10.1590/0366-69132020663802878>
- [27] J. Usman, M.H.D. Othman, A.F. Ismail, M.A. Rahman, J. Jaafar, Y.O. Raji, A.O. Gbadamosi, T.H. El Badawy, K.A.M. Said, An overview of superhydrophobic ceramic membrane surface modification for oil-water separation, *J. Mater. Res. Technol.* (2021). <https://doi.org/10.1016/j.jmrt.2021.02.068>
- [28] Q. Gu, T.C.A. Ng, Q. Sun, A.M.K. Elshahawy, Z. Lyu, Z. He, L. Zhang, H.Y. Ng, K. Zeng, J. Wang, Heterogeneous ZIF-L membranes with improved hydrophilicity and anti-bacterial adhesion for potential application in water treatment, *RSC Adv.* 9 (2019) 1591–1601. <https://doi.org/10.1039/C8RA08758J>
- [29] D. Nevstrueva, A. Pihlajamäki, J. Nikkola, M. Mänttari, Effect of precipitation temperature on the properties of cellulose ultrafiltration membranes prepared via immersion precipitation with ionic liquid as solvent, *Membranes*. 8 (2018) 87. <https://doi.org/10.3390/membranes8040087>
- [30] M.M. Salman, N.S. Radhi, O.H. Sabr, H.T. Nhabih, Utilization of diverse cheap materials as pore generating agent to manufacture low-cost porous ceramic, *Cerâmica*. 66 (2020) 179–185. <https://doi.org/10.1590/0366-69132020663782873>
- [31] Z. Harun, T.C. Ong, T. Matsuura, S.K. Hubadillah, M.H.D. Othman, A.F. Ismail, Modelling of transport mechanisms and drying shrinkage for multilayer ceramic membrane structure, *Chem. Eng. Res. Des.* 133 (2018) 111–125. <https://doi.org/10.1016/j.cherd.2018.02.039>
- [32] O.V. Suvorova, E.A. Selivanova, J.A. Mikhailova, V.A. Masloboev, D.V. Makarov, Ceramic products from mining and metallurgical waste, *Appl. Sci.* 10 (2020) 3515. <https://doi.org/10.3390/app10103515>
- [33] S. Mankai, J. Madiouli, J. Sghaier, D. Lecomte, Determination of porosity from shrinkage curves during sintering of granular materials, *Dry. Technol.* 36 (2018) 557–566. <https://doi.org/10.1080/07373937.2017.1348358>
- [34] M.C. da Silva, H. de L. Lira, R. do C. de O. Lima, N.L. de Freitas, Effect of sintering temperature on membranes manufactured with clays for textile effluent treatment, *Adv. Mater. Sci. Eng.* 2015 (2015). <https://doi.org/10.1155/2015/371697>
- [35] H. Koonani, M. Amirnejad, Combined three mechanisms models for membrane fouling during microfiltration, *J. Membr. Sci. Res.* 5 (2019) 274–282. <https://doi.org/10.22079/jmsr.2019.95781.1224>
- [36] Norme Tunisienne NT. 106.002 : Norme Tunisienne NT. 106.002 (1989) relative aux rejets d'effluents dans le milieu hydrique (Protection de l'environnement). Norme homologuée par arrêté du Ministre de l'Economie Nationale du 20 juillet 1989, JORT no 59, page 1332. Date de prise d'effet: 1er octobre 1989, (1989). <http://www.citet.nat.tn/Portail/doc/SYRACUSE/40964/norme-tunisienne-nt-106-002-norme-tunisienne-nt-106-002-1989-relative-aux-rejets-d-effluents-dans-le> (accessed August 19, 2021).
- [37] D. Uçar, Membrane processes for the reuse of car washing wastewater, *J. Water Reuse Desalination*. 8 (2018) 169–175. <https://doi.org/10.2166/wrd.2017.036>
- [38] J. Torkashvand, H. Pasalari, M. Gholami, S. Younesi, V. Oskoei, M. Farzadkia, On-site carwash wastewater treatment and reuse: a systematic review, *Int. J. Environ. Anal. Chem.* (2020) 1–15. <https://doi.org/10.1080/03067319.2020.1772773>
- [39] M. Khemakhem, S. Khemakhem, R.B. Amar, Emulsion separation using hydrophobic grafted ceramic membranes by, *Colloids Surf. Physicochem. Eng. Asp.* 436 (2013) 402–407. <https://doi.org/10.1016/j.colsurfa.2013.05.073>
- [40] L. Shi, Y. Lei, J. Huang, Y. Shi, K. Yi, H. Zhou, Ultrafiltration of oil-in-water emulsions using ceramic membrane: Roles played by stabilized surfactants, *Colloids Surf. Physicochem. Eng. Asp.* 583 (2019) 123948. <https://doi.org/10.1016/j.colsurfa.2019.123948>
- [41] J. Wills, S. Moazzem, V. Jegatheesan, Treating Car Wash Wastewater by Ceramic Ultrafiltration Membranes for Reuse Purposes, in: M. Pannirselvam., L. Shu, G. Griffin, L. Philip, A. Natarajan, S. Hussain (eds.), *Water Scarcity Ways Reduce Impact*, Springer, Cham, 2019: pp. 63–73. https://doi.org/10.1007/978-3-319-75199-3_4
- [42] M.R. Jamalludin, S.K. Hubadillah, Z. Harun, M.H.D. Othman, M.Z. Yunus, Novel superhydrophobic and superoleophilic sugarcane green ceramic hollow fibre membrane as hybrid oil sorbent-separator of real oil and water mixture, *Mater. Lett.* 240 (2019) 136–139. <https://doi.org/10.1016/j.matlet.2018.12.111>
- [43] M. Abbasi, M. Mirfendereski, M. Nikbakht, M. Golshenas, T. Mohammadi, Performance study of mullite and mullite–alumina ceramic MF membranes for oily wastewaters treatment, *Desalination*. 259 (2010) 169–178. <http://dx.doi.org/10.1016/j.desal.2010.04.013>
- [44] S.K. Hubadillah, M.H.D. Othman, M.A. Rahman, A.F. Ismail, J. Jaafar, Preparation and characterization of inexpensive kaolin hollow fibre membrane (KHFM) prepared using phase inversion/sintering technique for the efficient separation of real oily wastewater, *Arabian J. Chem.* 13 (2020) 2349–2367. <https://doi.org/10.1016/j.matlet.2018.12.111>
- [45] D. Das, S. Baitalik, B. Haldar, R. Saha, N. Kayal, Preparation and characterization of macroporous SiC ceramic membrane for treatment of waste water, *J. Porous Mater.* 25 (2018) 1183–1193. <https://doi.org/10.1007/s10934-017-0528-5>